An electron-dominated lateral photovoltaic effect in ZnO-based perovskite heterojunction and its performance enhancement by pyro-phototronic effect

Haozhe Zhao, Siyang Guo, Zengkun Pu, Heqing Wen, Juan Wang, Jihong Liu*, Shufang Wang and Shuang Qiao *

Hebei Key Laboratory of Optic-Electronic Information and Materials, College of Physics Science and Technology, Hebei University, Baoding 071002, P. R. China.

* Corresponding authors. E-mail: liujihong@hbu.edu.cn, and sqiao@hbu.edu.cn

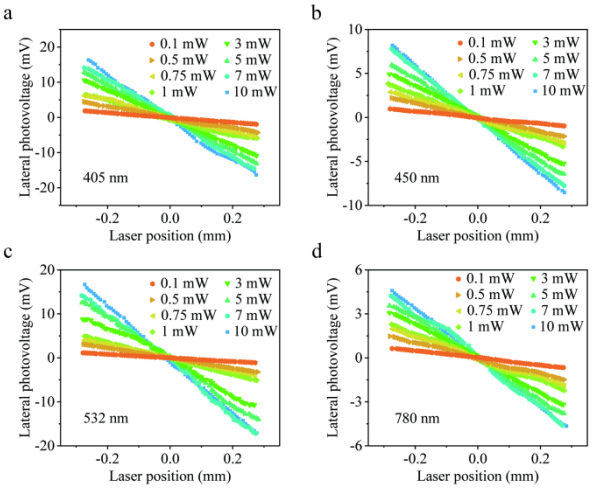

Fig. S1. Laser position-dependent LPV curves of the ZnO/PCBM/$MAPbI_3$ heterojunction PSD under the illumination of different powers with (a) 405 nm, (b) 450 nm, (c) 532 nm, and (d) 780 nm laser.

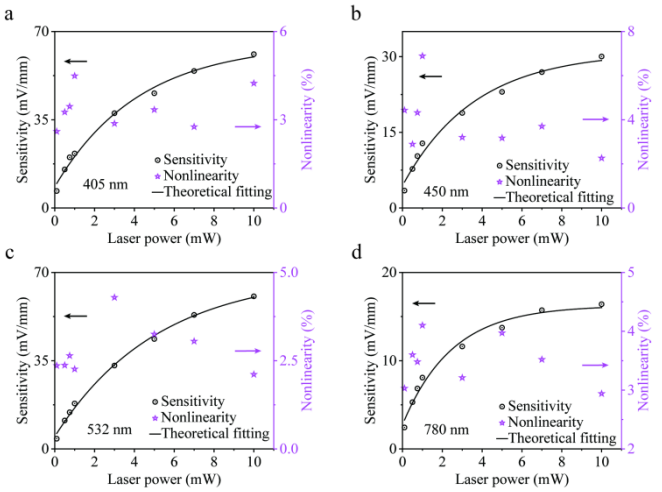

Fig. S2. Laser power-dependent sensitivities and nonlinearities curves of the ZnO/PCBM/$MAPbI_3$ heterojunction PSD under the illumination of different powers with (a) 405 nm, (b) 450 nm, (c) 532 nm, and (d) 780 nm laser.

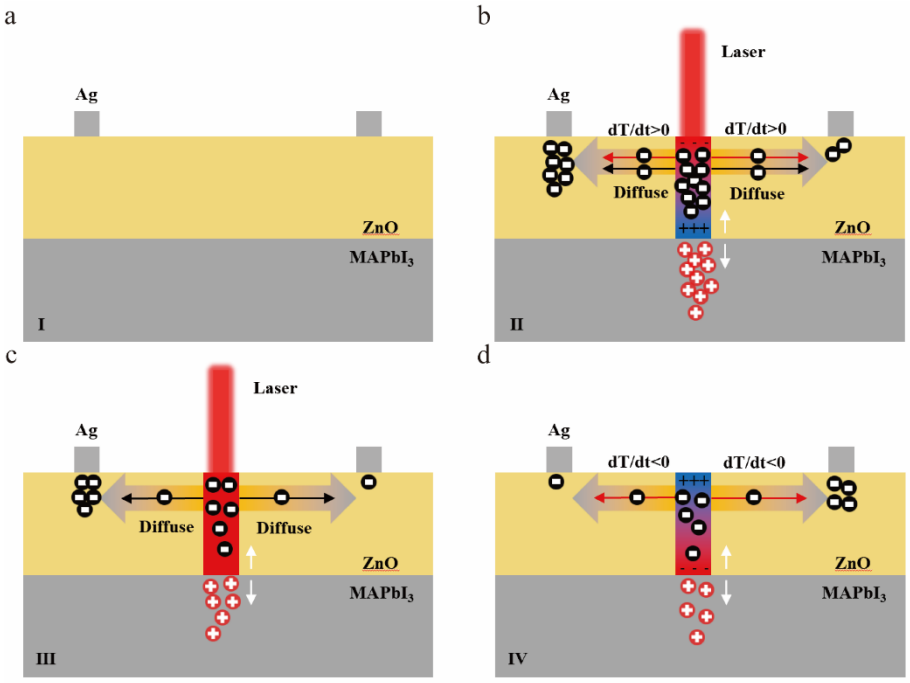

Fig. S3. The detailed working mechanism of LPV and pyroelectric effect enhanced LPV.

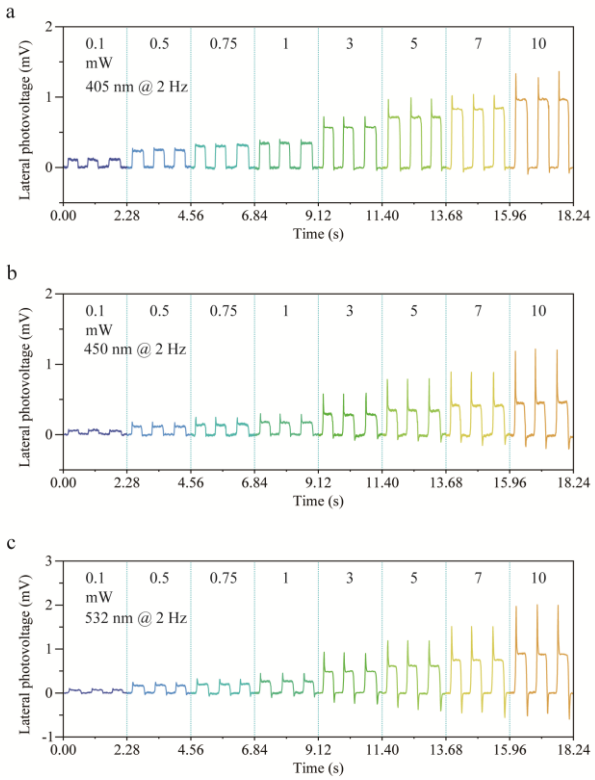

Fig. S4. Transient *LPV-t* curves of the ZnO/PCBM/$MAPbI_3$ heterojunction PSD under the illumination of different powers with (a) 405 nm, (b) 450 nm, and (c) 532 nm laser.

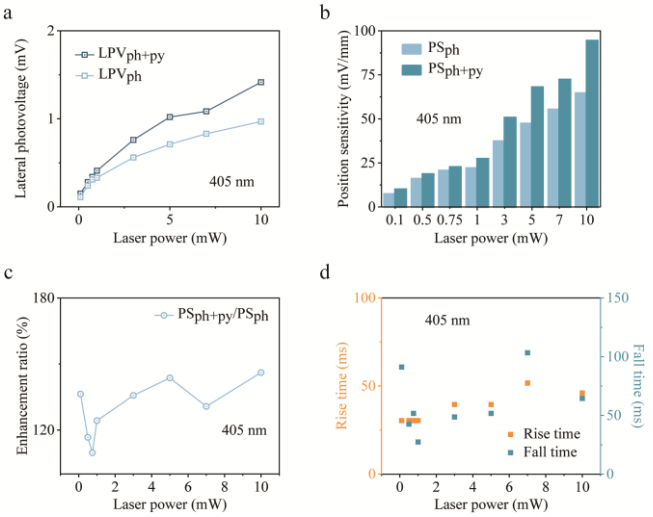

Fig. S5. (a) LPVs curves under the illumination of 405 nm laser at different powers. (b) PSs, (c) PS enhancement ratios and (d) rise time and fall time as a function of the laser power.

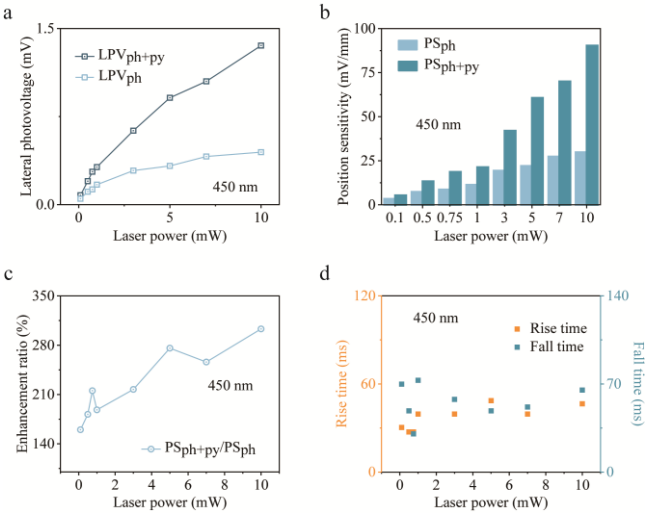

Fig. S6. (a) LPVs curves under the illumination of 450 nm laser at different powers. (b) PSs, (c) PS enhancement ratios and (d) rise time and fall time as a function of the laser power.

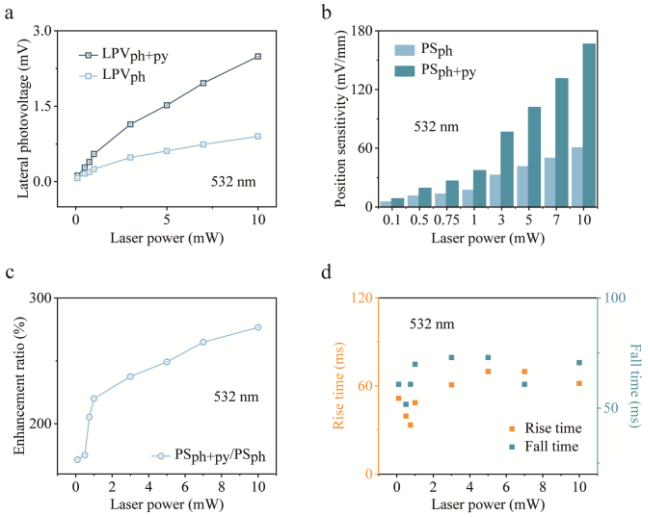

Fig. S7. (a) LPVs curves under the illumination of 532 nm laser at different powers. (b) PSs, (c) PS enhancement ratios and (d) rise time and fall time as a function of the laser power.

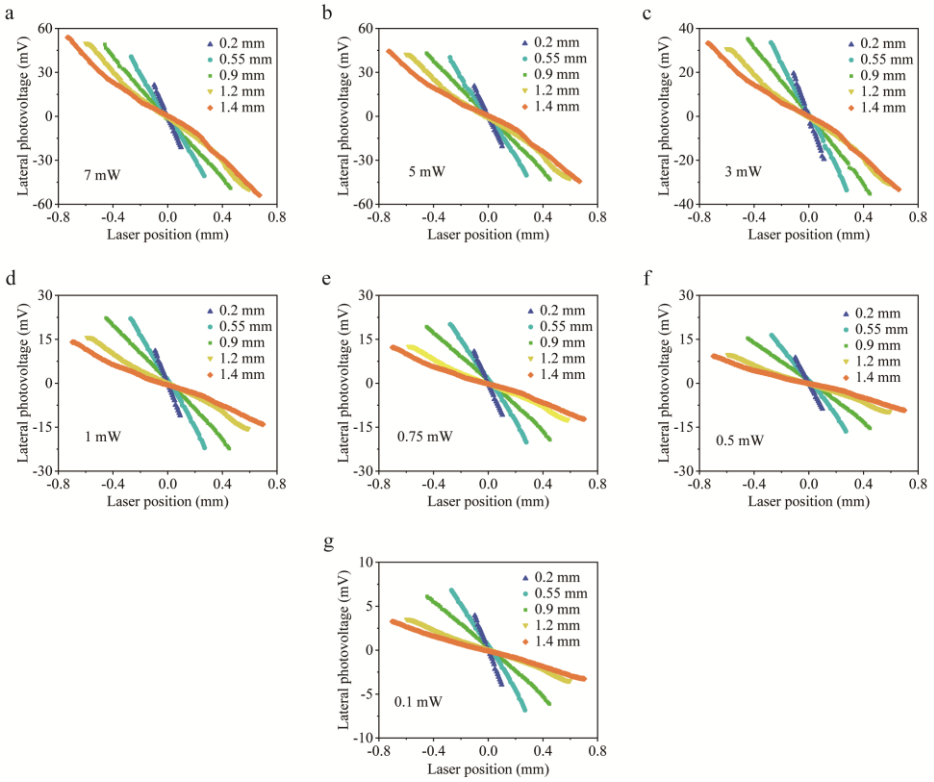

Fig. S8. Laser position-dependent LPV curves of the ZnO/PCBM/$MAPbI_3$ heterojunction PSD under the illumination of different electrode distances with (a) 7 mW, (b) 5 mW, (c) 3 mW, (d) 1 mW, (e) 0.75 mW, (f) 0.5 mW, and (g) 0.1 mW power.

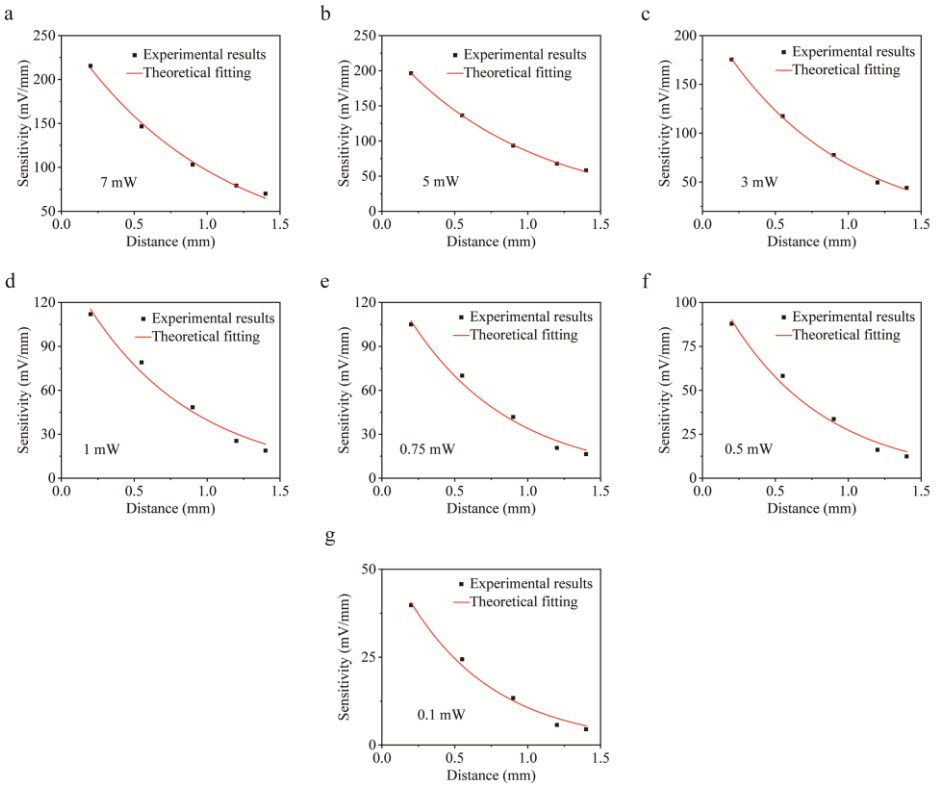

Fig. S9. Laser power-dependent sensitivities curves of the ZnO/PCBM/$MAPbI_3$ heterojunction PSD under the illumination of different electrode distances with (a) 7 mW, (b) 5 mW, (c) 3 mW, (d) 1 mW, (e) 0.75 mW, (f) 0.5 mW, and (g) 0.1 mW power.

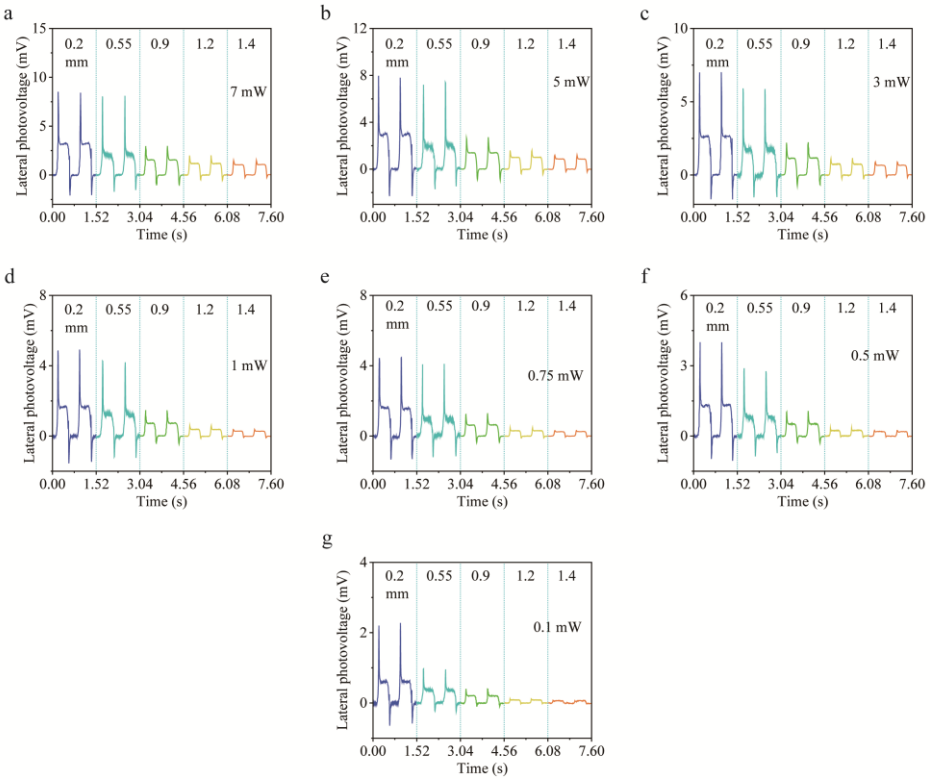

Fig. S10. Transient *LPV-t* curves of the ZnO/PCBM/$MAPbI_3$ heterojunction PSD under the illumination of different electrode distances with (a) 7 mW, (b) 5 mW, (c) 3 mW, (d) 1 mW, (e) 0.75 mW, (f) 0.5 mW, and (g) 0.1 mW power.

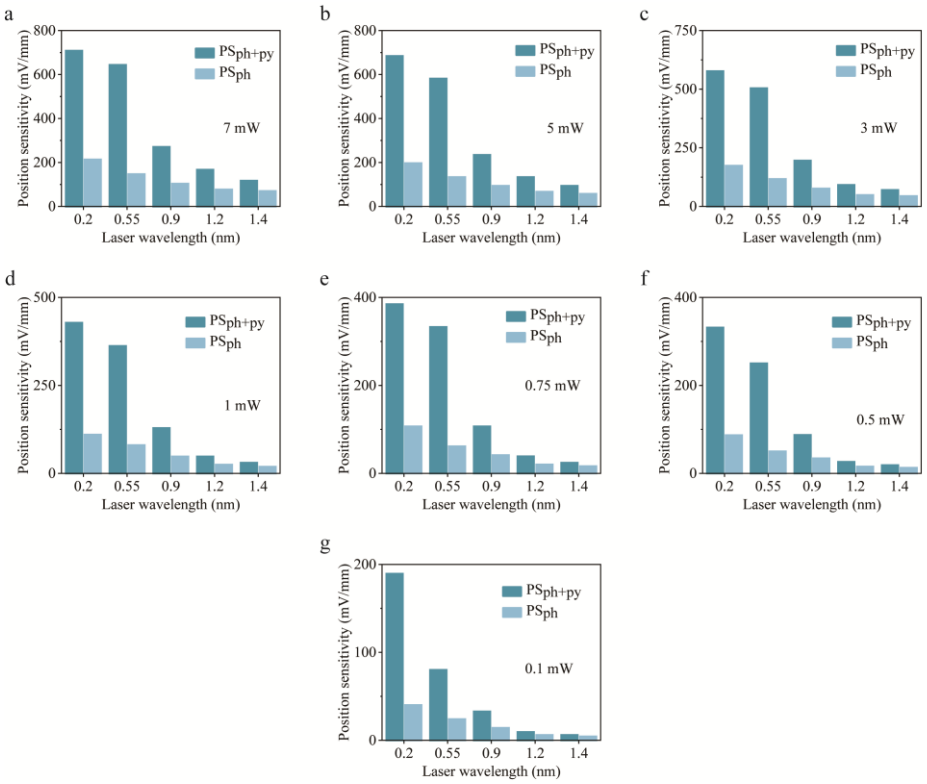

Fig. S11. PSs function of the ZnO/PCBM/$MAPbI_3$ heterojunction PSD under the illumination of different electrode distances with (a) 7 mW, (b) 5 mW, (c) 3 mW, (d) 1 mW, (e) 0.75 mW, (f) 0.5 mW, and (g) 0.1 mW power.

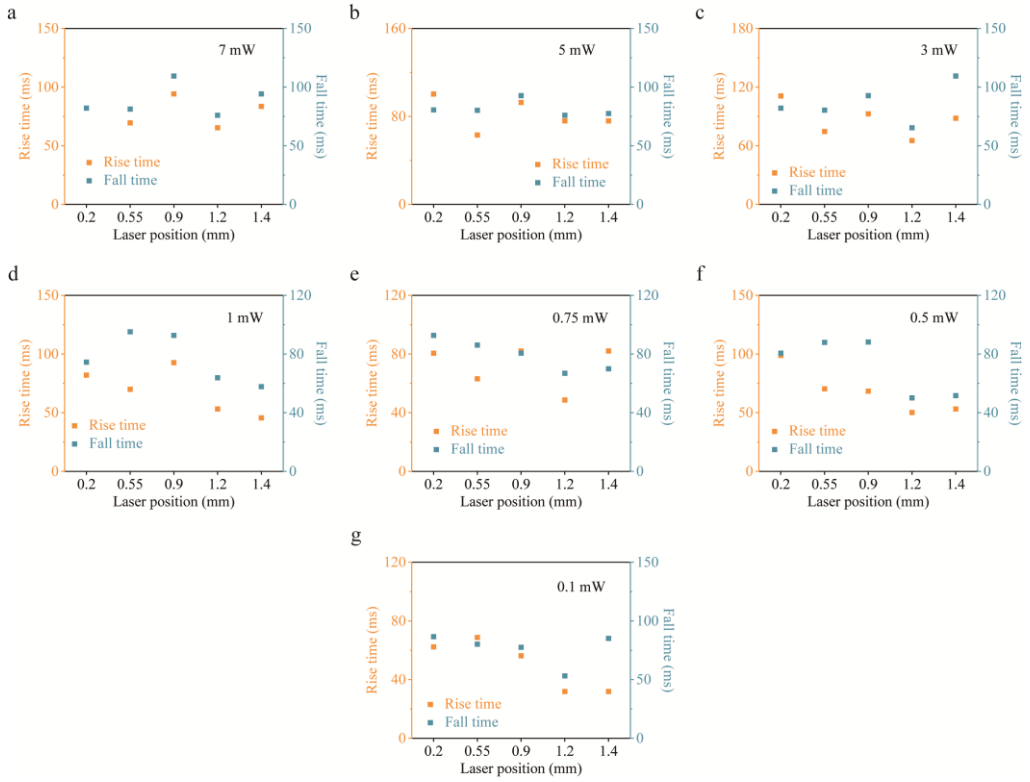

Fig. S12. Rise time and fall time function of the ZnO/PCBM/$MAPbI_3$ heterojunction PSD under the illumination of different electrode distances with (a) 7 mW, (b) 5 mW, (c) 3 mW, (d) 1 mW, (e) 0.75 mW, (f) 0.5 mW, and (g) 0.1 mW power.